5532 *Biochemistry* **2009,** *48,* 5532–5540
DOI: 10.1021/bi900139a

BIOCHEMISTRY
including biophysical chemistry & molecular biology
Article

Productive versus Unproductive Nucleotide Binding in Yeast Guanylate Kinase Mutants: Comparison of R41M with K14M by Proton Two Dimensional Transferred NOESY[†]

Bruce D. Ray,[‡] Joshua Scott,[‡] Honggao Yan,[⊥] and B. D. Nageswara Rao*,[‡]

[‡]*Department of Physics, Indiana University - Purdue University at Indianapolis (IUPUI), 402 North Blackford Street, Indianapolis, Indiana 46202-3273, and* [⊥]*Department of Biochemistry and Molecular Biology, Michigan State University, East Lansing, Michigan 48824*

Received January 28, 2009; Revised Manuscript Received May 5, 2009

ABSTRACT: The R41M and K14M mutant enzymes of yeast guanylate kinase (GKy) were studied to investigate the effects of these site-directed mutations on bound-substrate conformations. Published X-ray crystal structures of yeast guanylate kinase indicate that K14 is part of the "P" loop involved in ATP and ADP binding, while R41 is suggested as a hydrogen bonding partner for the phosphoryl moiety of GMP. Both of these residues might be involved in transition state stabilization. Adenosine conformations of ATP and ADP and guanosine conformations of GMP bound to R41M and K14M mutant yeast guanylate kinase in the complexes GKy·MgATP, GKy·MgADP, and GKy·MgADP·[u-^{13}C]GMP were determined by two-dimensional transferred nuclear Overhauser effect (TRNOESY) measurements combined with molecular dynamics simulations, and these conformations were compared with previously published conformations for the wild type. In the fully constrained, two substrate complexes, GKy·MgADP·[u-^{13}C]GMP, the guanyl glycosidic torsion angle, χ, is 51 ± 5° for R41M and 47 ± 5° for K14M. Both are similar to the published 50 ± 5° published for wild type. For R41M with adenyl nucleotides, the glycosidic torsion angle, χ, was 55 ± 5° with MgATP, and 47 ± 5° with MgADP, which compares well to the 54 ± 5° published for wild type. However, for K14M with adenyl nucleotides, the glycosidic torsion angle was 30 ± 5° with MgATP and 28 ± 5° with MgADP. The results indicate that bound adenyl-nucleotides have significantly different conformations in the wild-type and K14M mutant enzymes, suggesting that K14 plays an important role in orienting the triphosphate of MgATP for catalysis.

Because transfer of the terminal phosphoryl moiety from one mononucleotide to another, or from a mononucleotide either to a small molecule or to a protein substrate, plays a fundamental role in a number of aspects of metabolism, in signal transduction, and in gene regulation, much study has been invested in how kinases transfer phosphoryl groups (*1*). A synergistic interaction between site-directed mutagenesis, X-ray crystallography, and NMR[1] spectroscopy has been found exceedingly helpful in elucidating structural concomitants of phosphoryl group transfer (*2*). An important component of the synergy has been determination of the degree of structural perturbation that results from a mutation, particularly in the substrate binding conformations. NMR has proven to be a useful experimental technique for solution phase determination of bound substrate conformations and distances of traversal of itinerant moieties (*3*−*9*). Productive conformations for a bisubstrate reaction are characterized by geometrical constraints such as the relative orientation of moieties within each bound substrate, the relative orientation of bound substrates with respect to each other, the orientation of each bound substrate with respect to the critical moieties of the enzyme, the traversal distances of itinerant substrate moieties, and other aspects regarding the topography of the active site.

Guanylate kinase, by SCOP classification a member of the nucleotide and nucleoside kinases family in the P-loop containing nucleotide triphosphate hydrolases superfamily (*10*), is a small, typically monomeric enzyme that catalyzes the reversible reaction

$$\mathrm{MgATP} + \mathrm{GMP} \leftrightarrows \mathrm{MgADP} + \mathrm{GDP} \qquad (1)$$

similar to the adenylate kinase reaction (*11*, *12*). At 20.5 kDa, yeast GK is part of a short sequence subfamily that lacks a full lid domain. Guanylate kinase's essential role in conversion of GMP to GDP gives it a critical role in GTP biosynthesis. Consequently, cellular functions that involve GTP such as the control of the cGMP cycle (*13*) are affected by GK. GKs participation in the activation of antiviral acyclic guanosine

[†]Supported in part by National Institutes of Health (GM43966 and GM51901) and IUPUI.

*To whom correspondence should be addressed. Street address: 402 N. Blackford St., Rm. LD-154. Phone: (317) 274-6897. Fax: (317) 274-2393. E-mail: brao@iupui.edu.

[1]Abbreviations: 2D, two-dimensional; ADP, adenosine-5′-diphosphate; ATP, adenosine 5′-triphosphate; GK, guanylate kinase; GKy, cloned yeast guanylate kinase, GMP, guanosine 5′-monophosphate; MD, molecular dynamics; NMR, nuclear magnetic resonance; NOE, nuclear Overhauser effect; PDB, protein data bank; rmsd, root mean squared deviation; Tris-d_{11}, deuterated tris(hydroxymethyl)aminomethane; TRNOESY, transferred two-dimensional nuclear Overhauser effect spectroscopy.

 Published on Web 05/06/2009

analogues is a pharmacological consequence of its role in GTP biosynthesis (*14*−*16*), whose biomedical role has attracted attention to the structure and function of guanylate kinase.

Prior NMR studies of changes in bound substrate conformations between wild type and Y78F mutant GKy suggested significant perturbation of the glycosidic angle of bound GMP in the E·MgADP·GMP complex (*3*). Because of this significant perturbation on the substrate conformation, any straightforward mechanistic interpretation of kinetic and binding constant measurements of this mutant becomes less certain. Furthermore, this observation raises some additional questions. Because the hydroxyl of Y78 provides a hydrogen bond to the GMP phosphate, the perturbation observed might be a general effect of interference with hydrogen bonding to the phosphate. On the other hand, maintaining the bound GMP in a certain conformation might be a specific function of the hydroxyl of Y78. Finally, it might be an artifact of mutations within the GMP binding site not to be replicated in other nucleotide binding sites. Thus, the generality both of the observation, and of the method, need further examination with some well-selected GKy mutants. Furthermore, structural perturbation in this context should encompass the protein as well as the bound substrates.

In yeast guanylate kinase, K14 is the "invariant lysine" of the canonical "P-loop" or Walker A (*17*) motif, GXXXXGKT/S, located in what is termed the core region of the enzyme (*18*−*20*). In contrast, R41 is part of the nucleotide monophosphate binding domain that contributes a hydrogen bond to the phosphoryl moiety of GMP (*18*, *20*). Figure 1 shows the relative locations and orientations of K14 and R41 with respect to bound GMP as seen in X-ray crystallography (*20*). This paper presents a comparison of adenyl and guanyl conformations of enzyme-bound nucleotides with the K14M and R41M mutant enzyme of yeast guanylate kinase by means of TRNOESY.

EXPERIMENTAL PROCEDURES

Materials. GMP, ADP, ATP, tris(hydroxymethyl)aminomethane, and Sephadex G-75 were purchased from Sigma, DEAE-cellulose from Whatman, Blue Sepharose resin from Pharmacia, Hepes from Research Organics, and Chelex-100 from Bio-Rad. Deuterated tris(hydroxymethyl)aminomethane (Tris-d_{11}), 99.96% D_2O, and sodium [2,2,3,3-D_4]trimethylsilylpropionate (TMSP) were from Cambridge Isotope Laboratories. [u-^{13}C]GMP was from Spectra Stable Isotopes. All other chemicals were reagent grade.

Sample Preparation. Preparation of expression systems, and purification for both R41M and K14M mutant enzymes, were performed according to previously published procedures for wild type GKy (*12*). To further reduce adenylate kinase contamination, the resultant enzyme solutions were passed over DEAE-cellulose equilibrated with 30 mM Tris-HCl, pH 7.5 to which adenylate kinase binds and GKy does not (*11*). Enzyme purities were assessed by electrophoresis, and specific activities were assayed by monitoring ADP and GDP formation in a coupled assay with pyruvate kinase and lactate dehydrogenase (*11*, *12*, *21*, *23*). At room temperature, the specific activity is typically 2.0 units/mg for the R41M mutant, and 4.2 units/mg for the K14M mutant compared to 400 units/mg for the wild type.

Enzyme solutions were prepared for TRNOESY by conzcentrating the enzyme to ~50 mg/mL in an Amicon ultrafiltration concentrator with a YM10 membrane (molecular weight cutoff of 10000) and exchanging the buffer with 30 mM Tris-d_{11}, 150 mM KCl, 20 mM 2-mercaptoethanol, pH 7.5 in D_2O by repeated concentrations in a 10 mL Amicon concentrator. Nucleotides were prepared by dissolving in D_2O, adjusting to pH 8.0, and passing through a Chelex-100 column to remove contaminating metal ions. Nucleotide solutions were then lyophilized, redissolved in D_2O, and stored at −20 °C until needed. Concentrations of nucleotides and enzymes were determined spectrophotometrically with extinction coefficients ε_{259}^{mM} = 15.4 cm^{-1} for ADP and ATP, ε_{252}^{mM} = 13.8 cm^{-1} for GMP, and $\varepsilon_{280}^{mg/mL}$ = 0.741 cm^{-1} for both Gky enzymes (molecular mass, 20 550 Da) (*12*). All buffer solutions were passed through Chelex-100 to remove trace metal ion impurities, and pH values were not corrected for D_2O isotope effects.

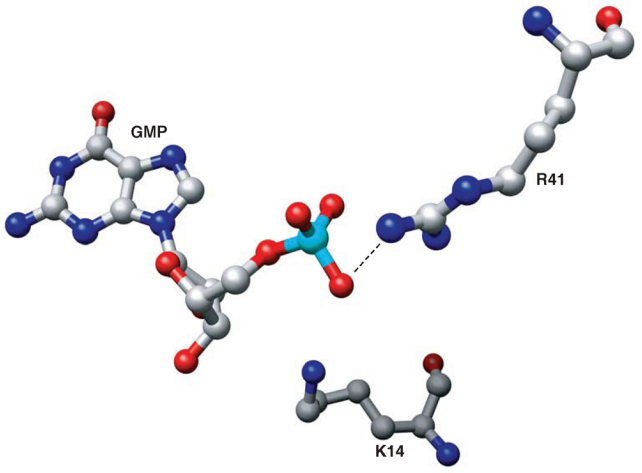

FIGURE 1: Relative locations of K14 and R41 with respect to GMP as revealed by X-ray crystallography (*21*). The R41 guanidino-GMP phosphate hydrogen bond is indicated by the dashed line. This figure was produced using the UCSF Chimera package from the Computer Graphics Laboratory, University of California, San Francisco, CA (supported by NIH Grant P41 RR-01081) (*22*).

NMR Measurements. All TRNOESY measurements were made at 5 °C on a Varian Inova-500 NMR spectrometer at the IUPUI NMR Center. A typical sample composition was 3 mM nucleotide, 0.3 mM GKy, 7 mM $MgCl_2$, and 8 mM 2-mercaptoethanol in 705 μL total volume.

NOESY data for E·MgATP and E·MgADP complexes were acquired in hypercomplex mode (*24*) with a 2K (t_2) × 256 (t_1) complex points data size for mixing times from 30 to 200 ms. For each t_1 increment, 16 scans and a relaxation delay of 2 s were used. Zero quantum interference was suppressed by random variation of the mixing time up to 10% of its value between different t_1 increments (*25*). In all experiments, the carrier frequency was placed 2 Hz to low field of the HDO resonance, and the solvent resonance was suppressed by monochromatic irradiation using the decoupler channel during the relaxation delay, t_1, and mixing periods. Data points were extended by linear prediction in both dimensions followed by Gaussian apodizations to give 4K (F_2) × 1K (F_1) complex points transformed data sets.

Gradient coherence selected ^{13}C-HSQC-NOESY data for E·MgADP·[u-^{13}C]GMP complexes were acquired in hypercomplex mode (*24*) with a 2K (t_2) × 128 (t_1) complex points data size for mixing times from 30 to 200 ms and without any further efforts to suppress either zero quantum interference or the solvent resonance. In these experiments, the carrier frequency was placed exactly on the HDO resonance, and 64 scans were recorded at each t_1 increment with a relaxation delay of 0.8 s. These data

points were also extended by linear prediction in both dimensions followed by Gaussian apodizations to give 4K (F_2) × 1K (F_1) complex points transformed data sets.

Theoretical Details. The basic theory of TRNOESY can be found in many publications (*26*−*31*). It has been shown that under fast-exchange conditions, that is, τ_b^{-1}, $\tau_f^{-1} \gg (\mathbf{W}_b)_{ij}$, $(\mathbf{W}_f)_{ij}$, for times greater than $(\tau_b^{-1} + \tau_f^{-1})^{-1}$, the time evolution of the longitudinal magnetizations of an n-spin system is given by (*31*):

$$\frac{d}{dt}(\mathbf{m}_b + \mathbf{m}_f) \approx -\mathbf{R}(\mathbf{m}_b + \mathbf{m}_f) \approx -(p_b\mathbf{W}_b + p_f\mathbf{W}_f)(\mathbf{m}_b + \mathbf{m}_f) \quad (2)$$

where the subscripts b and f refer to bound state and free state, respectively, p_b and p_f are population fractions of the ligand, $\mathbf{m}_b$ and $\mathbf{m}_f$ are *n*-dimensional vectors with each element representing the deviation of the *z*-magnetization of a spin from its equilibrium value, $\mathbf{W}_b$ and $\mathbf{W}_f$ are *n* x *n* relaxation matrices, and τ_b and τ_f are the lifetimes of the bound and free states respectively. For homonuclear spin systems, if dipolar interaction is the only relaxation mechanism, the relaxation matrix elements of $\mathbf{W}_b$ and $\mathbf{W}_f$ are given by standard expressions (*31*−*33*):

$$\mathbf{W}_{ii} = \frac{\gamma^4\hbar^2\tau_c}{10}\left[1 + \frac{3}{1+\omega^2\tau_c^2} + \frac{6}{1+4\omega^2\tau_c^2}\right]\sum_{k\neq i} r_{ik}^{-6} \quad (3)$$

$$\mathbf{W}_{ij} = \mathbf{W}_{ji} = \frac{\gamma^4\hbar^2\tau_c}{10r_{ij}^6}\left[-1 + \frac{6}{1+4\omega^2\tau_c^2}\right] \quad (4)$$

where γ and ω are the gyromagnetic ratio and Larmor frequency of the protons, r_{ij} is the distance between spin *i* and spin *j*, and τ_c is the isotropic rotational correlation time. r_{ij} and τ_c will correspond to free and bound species depending on whether $\mathbf{W}_b$ or $\mathbf{W}_f$ is evaluated. Equations 3 and 4 assume that the spin system is in a single conformation characterized by the distances r_{ij}, and is undergoing isotropic rotational diffusion characterized by τ_c. The intensity of the $i \leftarrow j$ cross-peak in a two-dimensional (2D) TRNOESY experiment representing polarization transfer from *j* to *i*, for a mixing time τ_m, is given by (*4*):

$$m_{i\leftarrow j}(\tau_m) = (e^{-\mathbf{R}\tau_m})_{ij}M_{0j} = \left[\mathbf{I} - \mathbf{R}\tau_m + \frac{1}{2}\mathbf{R}^2{\tau_m}^2 - \frac{1}{6}\mathbf{R}^3{\tau_m}^3 + \cdots\right]_{ij} M_{0j} \quad (5)$$

where **I** is the $n \times n$ unit matrix. Equation 5 shows that, for short mixing times, the build-up of intensity of a cross-peak in a TRNOESY spectrum is a polynomial in τ_m, and the initial slope of the build-up curve is given by the linear term $\mathbf{R}_{ij}$. Since usually $\tau_c^b \sim 10$ ns, $\tau_c^f \sim 0.1$ ns, and $(\omega\tau_c^b)^2 \gg 1$, if 10% to 25% of the ligand is bound, so that $p_b \approx 0.1$−0.25, eqs 2 and 4 lead to

$$\mathbf{R}_{ij} \approx p_b(\mathbf{W}_b)_{ij} \approx -\frac{\gamma^4\hbar^2 p_b\tau_c^b}{10(r_{ij}^b)^6} \quad (6)$$

Therefore, the ratios of the initial slopes for spin pairs are related to the corresponding internuclear distances in the bound conformation by

$$\frac{\mathbf{R}_{ij}}{\mathbf{R}_{kl}} \approx \left(\frac{r_{kl}^b}{r_{ij}^b}\right)^6 \quad (7)$$

The distance r_{ij}^b can be estimated by using a calibration distance if such a distance can be identified within the spin system. For the nucleotide protons, the H1′−H2′ distance of 2.9 ± 0.2 Å, which remains practically unchanged for all sugar puckers and glycosidic torsions, is a convenient calibration distance and was used in the current work. $p_b\tau_c^b$ may be evaluated from eq 6. It may be seen that the cross-peak intensities in a TRNOESY spectrum for a ligand in fast exchange between bound and free forms are similar to those of an intact system with an effective correlation time given by $p_b\tau_c^b$. Spin diffusion effects are contained in the quadratic and higher order terms in eq 5 for a system of more than two spins.

Molecular Modeling. Energy minimizations were carried out on a Silicon Graphics Octane computer, running Irix 6.5.22, using the program SYBYL7.2 from Tripos Inc., St. Louis, MO. Tripos force field was used for all energy calculations, and the conjugate gradient algorithm was chosen for the minimization. Partial charges were estimated by the Gasteiger-Marsili method (*34*, *35*) with formal −1 charges assigned to phosphate hydroxyl oxygens and a +2 charge assigned to the divalent cation when it was included in the simulated system. Minimizations of pseudoenergy that included all NOE constraints derived from experimental data (accuracy ± 10%) were performed on MgATP, MgADP, and GMP (including the phosphate groups) in vacuo with a dielectric constant of 1.

Because H5′ and H5″ coalesce into a single resonance, the observed NOEs with H5′/H5″, such as H8−H5′/H5″, combines contributions from both H5′ and H5″. An average distance can be calculated by taking half the NOE buildup rate. If spin *i* has distances r_{i1} and r_{i2} from H5′ and H5″, respectively, this average distance, r_{iavg}, is related to r_{i1} and r_i by

$$r_{iavg} = \left(\frac{r_{i1}^{-6} + r_{i2}^{-6}}{2}\right)^{-1/6} \quad (8)$$

Except for the special case of $r_{i1} = r_{i2}$, r_{iavg} does not equal the distance from spin *i* to either H5′ or H5″. However, for $r_{i1} < r_{i2}$, we have $r_{i1} < r_{iavg} < r_{i2}$. Although r_{i1} and r_{i2} cannot be specified explicitly, their upper and lower bounds are limited to the maximum distance for observable NOEs, ∼5 Å (barring unusual spin-diffusion effects), and twice the van der Waals radius of protons, ∼1.8 Å. Therefore, in molecular modeling calculations, 1.8 Å $< r_{i1} < r_{iavg} < r_{i2} <$ 5 Å was used as a general constraint for H5′ and H5″ NOEs in which r_{i1} represented the shorter of the two distances from spin *i* to H5′/H5″ for $i = 8$.

In the energy minimization process using Sybyl, multiple starting coordinate sets are used out of which energetically and sterically acceptable minimized structures are identified. Typically, at least 80% of the minimized structures satisfy these criteria. Structural parameters, interproton distances and dihedral angles, are computed from the coordinates of these minimized structures and averaged to designate a model structure used for subsequent interpretation of the results.

RESULTS AND ANALYSIS

TRNOESY experiments were performed on E·Mg·ATP and E·Mg·ADP complexes of both the K14M and R41M mutant enzymes. Gradient coherence selected ^{13}C-HSQC-TRNOESY experiments were performed on E·Mg·ADP·[u-^{13}C]GMP complexes of both the K14M and R41M mutant enzymes. Sample conditions for the experiments appropriate to minimize

effects from nonspecific binding were determined previously (*3*). On the basis of this, samples for experiments with these mutant enzymes contained 0.3 mM enzyme and 3 mM nucleotide, or nucleotides in the case of the two substrate complexes measured by gradient coherence selected ^{13}C-HSQC-TRNOESY (*3*). The structure of adenosine with numbering of the protons and identification of the torsions of interest is given in Figure 2. Proton numbering and torsion identification are identical for guanyl nucleotides.

Difference Spectra of Adenyl Nucleotide Complexes of Wild Type and K14M GKy. To detect site-directed mutation perturbations in the K21 M mutant enzyme of chicken muscle adenylate kinase, Tian et al.(*36*) compared the one-dimensional (1D) spectra of the wild type and mutant enzymes and observed significant alterations in the aromatic (8.5 to 6.0 ppm) and aliphatic (2.5 to 0.0 ppm) regions of the spectra with mutation. Such large alterations were not seen in this work either by 1D or by 2D spectroscopy.

Intramolecular NOEs of Adenyl-Nucleotides in K14M and R41M GKy-Bound Complexes. The H8−H2′ cross-peak was the strongest adenyl-nucleotide NOE cross-peak in 2D TRNOESY spectra of GKy-bound adenyl-nucleotides. This indicates that these adenyl-nucleotides bind in *anti* conformation. NOE buildups from nucleotide NOEs separable from the background protein intramolecular NOEs were used as constraints in molecular dynamics modeling. With unlabeled nucleotides, only three NOE buildups, H3′−H4′, H3′−H5′,5″, and H4′−H5′,5″, are obscured consistently by protein intramolecular NOEs. In all cases, NOEs between each of H8 and H1′ and each of the sugar protons were outside the protein background. The buildups of their NOEs were readily measurable and could provide distance constraints. Of course, overlapping cross-peaks occur for H8−H5′ and H8−H5″, as well as for H1′−H5′ and H1′−H5″.

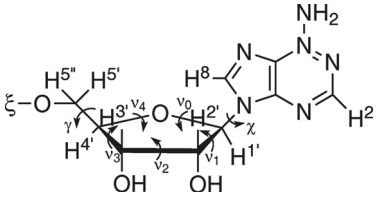

FIGURE 2: Chemical structure of adenosine moiety showing the numbering for the relevant protons and the torsion angles. Torsions are denoted as follows: χ (O4′−C1′−N9−C8), ν_0 (C4′−O4′−C1′−C2′), ν_1 (O4′−C1′−C2′−C3′), ν_2 (C1′−C2′−C3′−C4′), ν_3 (C2′−C3′−C4′−O4′), ν_4 (C3′−C4′−O4′−C1′), γ (O5′−C5′−C4′−C3′).

Table 1 shows distances computed from the TRNOESY data and distances fitted by molecular dynamics for both K14M and R41M mutant GKy complexes with MgATP compared with previously published data for wild type GKy complexes with MgATP. The interproton distances for the model for R41M were averaged over 19 structures (out of 25) deemed acceptable on the basis of agreement with experimental data, while for the model for K14M 21 out of 25 structures were used to derive the average. In both cases, the major violations occur for the H8−H5′ and H8−H5″ distances. Including H8−H5′ and H8−H5″, the rmsd values for the distance data are 0.26 Å for R41M and 0.44 Å for K14M. The rmsd of the glycosidic torsion is 5.0° for R41M and 3.1°, for K14M while the rmsd for the dihedral angles of the sugar was 9.9° for R41M and 15.7° for K14M.

Both mutants bind MgATP nearly equally well, although neither binds MgATP as well as wild type. While R41 is implicated in a hydrogen bond to the GMP phosphate, K14 is in the P-loop where the adenyl-nucleotide phosphates are presumed to bind. For each mutant enzyme, the major difference between modeled conformations in energy minimizations for that mutant enzyme were related to the C4′−C5′ sugar dihedral angle, γ, shown in Table 2. Although in both cases this angle is only constrained by NOE data involving H5′,5″, the data might represent a real difference in the orientation of the phosphate chain in the respective complexes. In contrast, the glycosidic torsion, χ, is constrained well by the NOE data. With R41M, the glycosidic torsion for bound MgATP is 55 ± 5°, virtually identical to the 54 ± 5° reported for the wild type. However, with K14M the glycosidic torsion is 30 ± 5°, quite noticeably different from that reported for wild type. Thus, for the R41M mutant enzyme, the sugar and base are bound very similarly to the wild type, but the K14M mutant enzyme clearly does not bind the sugar and base of MgATP in the same conformation as does the wild type.

Table 1: Interproton Distance Constraints for Adenosine Determined from Analyses of TRNOESY Data of R41M and K14M Mutant Gky in E·MgATP Complexes Compared to Wild Type (*3*)

	R41M		K14M		wild type	
distance	measured (±10%)	model (±0.3 Å)	measured (±10%)	model (±0.3 Å)	measured (±10%)	model (±0.3 Å)
H8−H1′	3.7	3.6	3.4	3.5	3.7	3.4
H8−H2′	2.6	2.4	2.9	2.7	2.7	2.7
H8−H3′	3.4	3.7	4.0	4.3	3.5	3.3
H8−H4′	3.9	4.2	3.7	4.0	3.2	3.7
H8−H5′	3.4[a]	2.1	4.6[a]	3.1	3.4[a]	2.8
H8−H5″	[a]	3.5	[a]	4.5	[a]	3.5
H1′−H2′	2.9	2.9	2.9	2.9	2.9	2.9
H1′−H3′	4.2	3.9	3.7	3.8	3.3	3.7
H1′−H4′	3.0	3.1	3.3	3.1	3.1	2.8
H1′−H5′	3.6[a]	3.8	4.3[a]	4.4	3.9[a]	3.7
H1′−H5″	[a]	4.4	[a]	5.1	[a]	4.6
H2′−H3′	2.3	2.3	2.5	2.4	2.2	2.3
H2′−H4′	4.0	4.0	3.5	3.7	[b]	3.8
H2′−H5′	2.9[a]	2.9	3.9[a]	3.8	2.9[a]	2.9
H2′−H5″	[a]	4.4	[a]	4.4	[a]	4.0
χ(O4′−C1′−N9−C8)		55 ± 5°		30 ± 5°		54 ± 5°

[a] This distance represents a nonlinear average of two NOE interactions (see the text). [b] Not detected.

Table 2: Mean Values (in degrees ±5°) of Various Torsion[a] Angles and Pseudorotation[b] Parameters of the Sugar Ring in the Calculated Structural Ensembles of GKy-Bound Nucleotides Compared to Wild Type (*3*)

	wild type (*3*)			K14M			R41M		
ang	E·Mg ATP	E·Mg ADP	E·Mg ADP·[u-^{13}C] GMP[c]	E·Mg ATP	E·Mg ADP	E·Mg ADP·[u-^{13}C] GMP[c]	E·Mg ATP	E·Mg ADP	E·Mg ADP·[u-^{13}C] GMP[c]
χ	54	53	50	30	28	47	55	47	51
ν_0	8	−4	−17	−27	−20	6	−14	−9	−25
ν_1	1	16	25	36	1	2	17	33	22
ν_2	−9	−20	−21	−28	17	−8	−13	−39	−10
ν_3	15	21	12	17	−30	12	5	35	−4
ν_4	−14	−11	3	5	34	−12	5	−17	17
P[d]	233	191	153	150	58	229	142	185	115
α[d]	15	20	24	33	32	12	16	39	24

[a] Torsions are denoted as follows: χ (O4′−C1′−N9−C8), ν_0 (C4′−O4′−C1′−C2′), ν_1 (O4′−C1′−C2′−C3′), ν_2 (C1′−C2′−C3′−C4′), ν_3 (C2′−C3′−C4′−O4′), ν_4 (C3′−C4′−O4′−C1′). [b] $P = \tan^{-1}[(\nu_4 + \nu_1) - (\nu_3 + \nu_0)/2\nu_2(\sin 36° + \sin 72°)]$; and $\alpha = \nu_2/\cos P$ are the phase angle and amplitude of pseudorotation of the sugar ring, respectively. When ν_2 is negative, 180° is added to the calculated value of P. [c] [u-^{13}C]GMP used in a ^{13}C selective TRNOESY to observe GMP resonances in the presence of overlapping resonances from [unlabeled]ADP. [d] Recomputed on the basis of the mean values before rounding of the sugar ring torsion angles.

Sugar puckers computed by molecular modeling, shown for the two complexes in columns 5 and 8 of Table 2, are similar but differ from the sugar pucker for the wild type enzyme shown in Table 2, column 2. On the basis of models of deoxynucleotides, it was shown that the dihedral angles determining sugar pucker are not particularly sensitive to ribose interproton distances other than H3′−H4′ and H1′−H4′ (*37*). In our experiments, of these two only H1′−H4′ gives a cross-peak separable from the protein background, and the modeled distances for this are the same for both R41M and K14M, but different from the modeled distance for the wild type enzyme. Thus, this difference, as well as the differences in some of the distances involving H8, indicates that the details of sugar pucker may be different from wild type for both these complexes with mutants. However, in view of the large rmsd values for the dihedral angles, differences in the values of the actual parameters used to characterize sugar pucker, P and α, are not likely to be accurate enough to be interpretable.

Table 3 shows distances computed from the TRNOESY data and distances fitted by molecular dynamics for both K14M and R41M mutant GKy complexes with MgADP compared with previously published data for wild type GKy complexes with MgADP. The interproton distances for the model for R41M were averaged over 24 structures deemed acceptable on the basis of agreement with experimental data (out of 25) while for the model for K14M 21 out of 25 structures were used to derive the average. In both cases, the major violations occur for the H8−H5′ and H8−H5″ distances. Including H8−H5′ and H8−H5″, the rmsd values for the distance data are 0.42 Å for R41M and 0.25 Å for K14M. The rmsd of the glycosidic torsion is 2.8° for R41M and 5.8° for K14M, while the rmsd for the dihedral angles of the sugar is 9.3° for R41M and 11.9° for K14M. As above, the glycosidic angles, χ, were well-constrained in the two mutant complexes. As expected, given the results with MgATP, the glycosidic torsion for the K14M·MgADP complex, 28 ± 5°, differed significantly from wild type's 53 ± 5°, while the same torsion for the R41M·MgADP complex, at 47 ± 5°, was similar to that for wild type. Thus, the point mutation at a site involved in adenyl-nucleotide binding, K14, alters the conformation of bound adenyl-nucleotides while the mutation at a site not suspected to be related to adenyl-nucleotide does not produce such an alteration. Again, differences in computed sugar puckers are seen, as shown in Table 2, columns 6 and 9. Comparison with wild type, shown in column 3 of the table, indicates that wild type and R41M may have the same sugar pucker for bound MgADP. However, the same limitation on interpretation of sugar pucker differences noted above applies here as well.

MgADP·[u-^{13}C]GMP Complexes with K14M and R41M Mutants of GKy. Prior NMR studies of GKy indicated that GMP binds at both nucleotide binding sites, while adenyl nucleotides cannot bind at the GMP binding site (*3*). MgADP was added to the GMP complexes to block the adenyl site from binding GMP, and an isotope selective experiment became necessary to eliminate interference from the MgADP sugar resonances (*3*). Table 4 shows distances computed from the TRNOESY data and distances fitted by molecular dynamics for [u-^{13}C]GMP in both K14M and R41M mutant GKy complexes compared with previously published data for wild type GKy with MgADP and [u-^{13}C]GMP (*3*). Because isotope selection suppresses the background resonances from the protein, more constraints are generated for bound GMP in these complexes. The interproton distances for the model for R41M were averaged over 24 structures deemed acceptable on the basis of agreement with experimental data (out of 25), while for the model for K14M 17 out of 25 structures were used to derive the average. Including H8−H5′ and H8−H5″, the rmsd values for the distance data are 0.21 Å for R41M and 0.49 Å for K14M. The rmsd of the glycosidic torsion is 0.4° for R41M and 1.6° for K14M, while the rmsd for the dihedral angles of the sugar was 1.2° for R41M and 2.2° for K14M.

There is very good convergence between the glycosidic torsion angles in the pseudoenergy minimization ensembles. For both mutant enzymes, within experimental error, the glycosidic torsions for bound GMP, 51 ± 5° for R41M and 47 ± 5° for K14M, are the same as found with wild type, 50 ± 5°. Although for both mutants GMP is not as tightly bound as in wild type, neither point mutation has altered the glycosidic torsion of bound GMP from that of wild type.

Mean values of sugar ring torsion angles and pseudorotation parameters obtained for GMP in E·MgADP·GMP for both mutant enzymes are given in columns 7 and 10 of Table 2 with the comparable values for wild type enzyme in column 4. The three complexes do show differences in sugar ring torsions, but it is not clear if the differences in sugar pucker between these complexes are interpretable.

Table 3: Interproton Distance Constraints for Adenosine Determined from Analyses of TRNOESY Data of R41M and K14M Mutant Gky in E·MgADP Complexes Compared to Wild Type (*3*)

	R41M		K14M		wild type	
distance	measured (±10%)	model (±0.3 Å)	measured (±10%)	model (±0.3 Å)	measured (±10%)	model (±0.3 Å)
H8−H1′	3.4	3.6	3.2	3.4	3.7	3.4
H8−H2′	2.3	2.2	2.9	3.1	2.7	2.6
H8−H3′	3.5	3.8	3.5	3.6	3.4	3.4
H8−H4′	3.5	3.7	4.4	4.4	2.9	3.4
H8−H5′	3.6[a]	2.3	4.4[a]	3.0	3.5[a]	3.1
H8−H5″	[a]	3.6	[a]	4.4	[a]	3.4
H1′−H2″	2.9	2.9	2.9	2.9	2.9	2.9
H1′−H3′	3.6	3.8	4.1	4.2	3.2	3.6
H1′−H4’	3.1	3.1	3.2	3.0	2.8	2.4
H1′−H5′	4.8[a]	4.5	4.2[a]	4.3	3.6[a]	3.8
H1′−H5″	[a]	5.0	[a]	4.6	[a]	4.4
H2′−H3′	2.2	2.1	2.7	2.5	2.4	2.1
H2′−H4′	2.8	3.2	3.3	3.6	2.6	2.9
H2′−H5′	2.9[a]	3.0	3.8[a]	3.9	2.9[a]	3.0
H2′−H5″	[a]	3.8	[a]	5.1	[a]	4.1
χ(O4′−C1′−N9−C8)		47 ± 5°		28 ± 5°		53 ± 5°

[a] This distance represents a nonlinear average of two NOE interactions (see text).

Table 4: Interproton Distance Constraints for Guanosine Determined from Analyses of TRNOESY Data of R41M and K14M Mutant Gky in E·MgADP·[u-^{13}C]GMP Complexes Compared to Wild Type (*3*)

	R41M		K14M		wild type (*3*)	
distance	measured (±10%)	model (±0.3 Å)	measured (±10%)	model (±0.3 Å)	measured (±10%)	model (±0.3 Å)
H8−H1′	3.7	3.5	3.3	3.6	3.1	3.5
H8−H2′	2.4	2.2	3.0	2.7	2.2	2.1
H8−H3′	2.7	2.9	3.4	3.4	2.9	3.3
H8−H4′	3.5	3.8	3.8	4.2	4.1	3.9
H8−H5′	3.4[a]	2.0	4.1[a]	2.2	3.8[a]	2.4
H8−H5″	[a]	3.4	[a]	3.9	[a]	3.8
H1′−H2′	2.9	3.0	2.9	2.9	2.9	2.9
H1′−H3′	3.5	3.7	3.9	4.1	3.4	3.8
H1′−H4’	2.9	2.8	3.8	3.4	3.1	3.0
H1′−H5′	3.9[a]	4.0	4.2[a]	4.2	[b]	4.4
H1′−H5″	[a]	4.5	[a]	4.7	[b]	4.5
H2′−H3′	2.0	2.1	2.3	2.2	2.0	2.0
H2′−H4′	[b]	3.9	3.5	3.7	2.8	3.3
H2′−H5′	2.9[a]	3.0	3.5[a]	3.7	2.9[a]	3.0
H2′−H5″	[a]	4.6	[a]	4.8	[a]	4.2
H3′−H4′	[b]	3.0	2.8	2.7	2.2	2.5
H3′−H5′	2.8[a]	2.1	3.7[a]	2.9	2.7[a]	2.5
H3′−H5″	[a]	3.5	[a]	3.7	[a]	3.4
H4′−H5′	2.4[a]	2.8	3.0[a]	2.9	2.2[a]	2.9
H4′−H5″	[a]	2.4	[a]	2.3	[a]	2.3
χ(O4′-C1′−N9-C8)		51 ± 5°		47 ± 5°		50 ± 5°

[a] This distance represents a nonlinear average of two NOE interactions (see text). [b] Not detected.

DISCUSSION

Site-directed mutagenesis is a powerful tool for studying structure−function relationships. However, the interpretation of the effects of site-directed mutagenesis is not without complications. Potential adverse effects of mutagenesis on the conformation of the protein have been well recognized, but the effects on bound substrate conformation are often neglected. NMR is a powerful yet facile tool for the determination of bound substrate conformation, particularly when the bound substrate is in fast exchange with the free. For enzymes that utilize nucleotides as substrates, comprehensive NMR methodologies making use of measurements of TRNOESY and paramagnetic relaxation enhancements for ^{31}P and ^{13}C nuclei in the substrates have yielded structural data for enzyme-bound nucleotides. These NMR structures often differ from those determined by X-ray crystallography. While crystallography data are typically the best source and usually the only source of structural data for amino-acid environments of ligands, there are reports of problems with structures of small molecule ligands in macromolecular refinement (*39*, *40*). Since the NMR data were obtained in solution, they are considered reliable for the bound substrates.

The TRNOESY analysis made here assumes that the NOEs represent a single conformation. This assumption has consequences both for experimental design and for interpretation.

Previous work laid out a stoichiometric control method by which contributions from weak, nonspecific binding can be minimized if not altogether removed (*4*). If more than one substrate conformation is operative at the specific binding site, the derived conformation will represent their weighted average. Since the NOE is proportional to the reciprocal sixth power of the interproton distance (r_{ij}^{-6}), if a given interproton distance is significantly different between two conformations, the averaging process would lead to a distorted inferred distance. These conformations would often be energetically unfavorable in the minimization process. In all our TRNOESY determinations of interproton distances in nucleotides, thus far, such situations have not arisen for base−sugar interproton distances. The most likely source for possible multiple conformations would be differences in sugar pucker. However, variations in interproton distances arising from sugar pucker are of low amplitude (*37*). Therefore, such an average is not likely to vitiate the assumption of single conformation.

In prior work, the glycosidic torsion angle for GMP (χ) in the wild type E·MgADP·[u-^{13}C]GMP complex was determined to be 50 ± 5° (*3*). With the R41M mutant enzyme, this glycosidic torsion angle is determined as 51 ± 5°, and with the K14M mutant enzyme, this glycosidic torsion angle is determined as 47 ± 5°. Neither mutation appears to affect the bound guanosine conformation even though R41 is a residue implicated in GMP binding. Note that this is in contrast to the previously published data for Y78F where the bound GMP conformation was strikingly different from that found in the wild type enzyme (*3*). Thus, while the results of the NMR conformational analysis suggested that the point mutation altered the bound GMP conformation too greatly to permit the quantification of the contribution of Y78 to GK catalysis, the data for R41M presented here indicate that the kinetic data for this mutant can be interpreted with more confidence. K14 is not implicated in GMP binding, consistent with the observed lack of effect on GMP conformation in the E·MgADP·[u-^{13}C]GMP complex. Thus, mutation of residues hydrogen bonded to the GMP phosphate does not necessarily alter the glycosidic angle of bound GMP. This means that the effect observed with the Y78F mutant is specific to that mutation and not a general consequence of altering the hydrogen bonding of the GMP phosphoryl moiety.

In contrast, the difference with adenyl-nucleotides for these two mutant enzymes is striking. Consistent with the lack of involvement of R41 in adenyl-nucleotide binding, the glycosidic torsions obtained for MgATP, and for MgADP bound to the R41M mutant enzyme are like those seen with wild type. However, K14 is involved in adenyl-nucleotide binding, and the glycosidic torsions with K14M obtained for MgATP, and for MgADP (30 ± 5°, and 28 ± 5°, respectively) are strikingly different from the 54 ± 5° and 53 ± 5°, respectively, previously published for the wild type enzyme (*3*). This change suggests a link between the binding effects of the K14M mutation and the diminished enzyme activity of the mutant. Figure 3 gives a comparison of the orientations of the base in wild type and K14M mutant enzyme complexes.

In chicken muscle adenylate kinase, K21 is the lysine that corresponds to K14 in yeast guanylate kinase. Substantial conformational changes from the wild type enzyme consistent with global conformational effects were reported for the K21 M mutant of chicken muscle adenylate kinase (*36*). However, for the K21A mutant chicken muscle adenylate kinase,

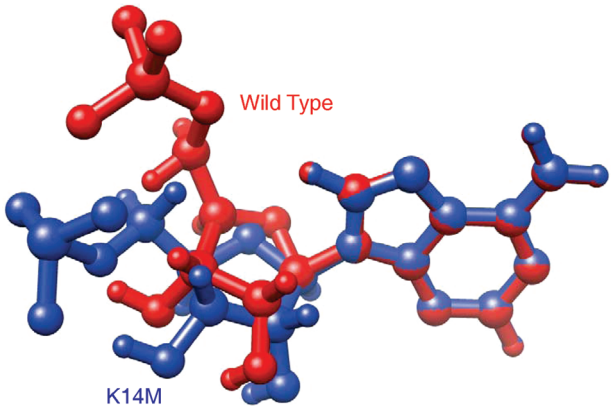

FIGURE 3: Comparison of conformations of ADP in the E·MgADP complex for wild type (red) and K14M mutant (blue) GKy. Each of the structures drawn represents one of the acceptable structures obtained for the respective complex by energy minimization.

a nonconservative mutation, conformational perturbations were limited (*38*). Results of the conservative mutation of chicken muscle adenylate kinase, K21R, indicated that the protein conformational changes were more than just an effect of side chain charge (*38*). As noted above, in contrast to the case with chicken muscle adenylate kinase, NMR did not give any evidence of protein conformational changes between the K14M mutant of yeast guanylate kinase and wild type enzyme. It should be noted that that each and every protein conformational alteration may not be NMR sensitive.

On the basis of ^{1}H NMR observed protein conformational changes with mutations to E43 of staphylococcal nuclease, Hilber and co-workers warned future investigators to be sure that site-directed mutations do not alter protein conformation before attempting quantitative interpretation of kinetic parameters obtained from such mutants (*41*). The current work suggests that the lack of large-scale protein conformational changes, while necessary, is not sufficient to ensure a meaningful quantitative interpretation of kinetic parameters obtained from site-directed mutants. In addition, evidence that the conformations of the bound substrates are not significantly disturbed must be obtained. For small molecule ligands at least, for a number of documented reasons (*39*, *40*), accurate determination of critical conformational parameters such as dihedral angles may require solution state structural techniques such as NMR.

Interestingly, the deviation in adenyl-nucleotide glycosidic torsion for the K14M mutant enzyme is in the opposite direction from the deviation of the guanyl-nucleotide glycosidic torsion previously published for the Y78F mutant enzyme (*3*). Tyrosine 78 is located above the plane of the GMP ribosyl ring and on the same side as the guanyl moiety. Motion of the more hydrophobic phenylalanine away from the charged environment around the phosphate would tend to push the guanyl moiety farther away from the ribosyl O4′ increasing the glycosidic angle. In contrast, K14 is involved in phosphate orientation and is located near the adenyl-nucleotide β-phosphate. Thus, in the K14M mutant enzyme, the sugar is pushed so as to decrease the glycosidic angle.

P-loop is the most frequently occurring motif among kinases and nucleotide phosphatases (*42*). The functional importance of the invariant lysine in the P-loop has been demonstrated by numerous site-directed mutagenesis studies, but few studies have investigated its exact role in catalysis. By ^{31}P NMR, Tsai and co-workers show that the bound conformations of the phosphate

chain of the bisubstrate analogue, P^1,P^5-bis(5′-adenosyl)pentaphosphate, in the wild-type chicken muscle adenylate kinase and the invariant lysine mutant enzymes are different and suggest that the functional role of the invariant Lys is to orient the triphosphate chain of MgATP to a proper conformation required for catalysis. In this study, by TRNOESY, we show that the glycosidic torsion angles of the bound MgATP or MgADP in the wild-type GKy and the K14M mutant enzyme are significantly different (*38*). If it is assumed for simplicity that the positions of the adenine moiety in the wild-type and mutant enzymes are the same, the conformations of the phosphate chain must be significantly different between the wild-type and mutant enzymes (Figure 3). Such a variation, taken in conjunction with X-ray data on the position of K14 in GKy (*11*, *18*, *20*), as well as with the results from NMR studies on adenylate kinase (*38*), suggests that the functional role of K14 in GKy is similar to that of K21 in chicken muscle adenylate kinase in facilitating the appropriate orientation of the triphosphate chain of MgATP for phosphoryl transfer. This may be a role shared by the invariant lysine in the P-loops of other kinases.

REFERENCES

1. Matte, A., Tari, L. W., and Delbaere, L. T. J. (1998) How Do Kinases Transfer Phosphoryl Groups?. *Structure 6*, 413–419.
2. Tsai, M.-D, and Yan, H. (1991) Mechanism of Adenylate Kinase: Site-Directed Mutagenesis versus X-ray and NMR. *Biochemistry 30*, 6806–6818.
3. Ray, B. D., Jarori, G. K., Raghunathan, V., Yan, H., and Nageswara Rao, B. D. (2005) Conformations of Nucleotides Bound to Wild Type and Y78F Mutant Yeast Guanylate Kinase: Proton Two-Dimensional Transferred NOESY Measurements. *Biochemistry 44*, 13763–13770.
4. Murali, N., Jarori, G. K., Landy, S. B., and Nageswara Rao, B. D. (1993) Two-Dimensional Transferred Nuclear Overhauser Effect Spectroscopy (TRNOESY) Studies of Nucleotide Conformations in Creatine Kinase Complexes: Effects Due to Weak Nonspecific Binding. *Biochemistry 32*, 12941–12948.
5. Murali, N., Jarori, G. K., and Nageswara Rao, B. D. (1994) Two-Dimensional Transferred Nuclear Overhauser Effect Spectroscopy Study of the Conformation of MgATP Bound at the Active and Ancillary Sites of Rabbit Muscle Pyruvate Kinase. *Biochemistry 33*, 14227–14236.
6. Jarori, G. K., Murali, N., and Nageswara Rao, B. D. (1994) Two-Dimensional Transferred Nuclear Overhauser Effect Spectroscopy (TRNOESY) Studies of Nucleotide Conformations in Arginine Kinase Complexes. *Biochemistry 33*, 6784–6791.
7. Murali, N., Lin, Y., Mechulam, Y., Plateau, P., and Nageswara Rao, B. D. (1997) Adenosine Conformations of Nucleotides Bound to Methionyl tRNA Synthetase by Transferred Nuclear Overhauser Effect Spectroscopy. *Biophys. J. 70*, 2275–2284.
8. Jarori, G. K., Murali, N., Switzer, R. L., and Nageswara Rao, B. D. (1995) Conformation of MgATP Bound To 5-Phospho-α-D-Ribose 1-Diphosphate Synthetase by Two-Dimensional Transferred Nuclear Overhauser Effect Spectroscopy. *Eur. J. Biochem. 230*, 517–524.
9. Lin, Y., and Nageswara Rao, B. D. (2000) Structural Characterization of Adenine Nucleotides Bound to *Escherichia coli* Adenylate Kinase. 1. Adenosine Conformations by Proton Two-Dimensional Transferred Nuclear Overhauser Spectroscopy. *Biochemistry 39*, 3636–3646.
10. Cheek, S., Zhang, H., and Grishin, N. V. (2002) Sequence and Structure Classification of Kinases. *J. Mol. Biol. 320*, 855–881.
11. Berger, A, Schiltz, E., and Schulz, G. E. (1989) Guanylate Kinase from *Saccharomyces cerevisiae*: Isolation and Characterization, Crystallization and Preliminary X-ray Analysis, Amino Acid Sequence and Comparison with Adenylate Kinases. *Eur. J. Biochem. 184*, 433–443.
12. Li, Y., Zhang, Y., and Yan, H. (1996) Kinetic and Thermodynamic Characterizations of Yeast Guanylate Kinase. *J. Biol. Chem. 271*, 28038–28044.
13. Hall, S. W., and Kuhn, H. (1986) Purification and Properties of Guanylate Kinase from Bovine Retinas and Rod Outer Segments. *Eur. J. Biochem. 161*, 551–556.
14. Miller, R. L., and Miller, W. H. (1980) Phosphorylation of Acyclovir (Acycloguanosine) Monophosphate by GMP Kinase. *J. Biol. Chem. 255*, 7204–7207.
15. Boehme, R. E. (1984) Phosphorylation of the Antiviral Precursor 9-(1,3-Dihydroxy-2-propoxymethyl)guanine Monophosphate by Guanylate Kinase Isozymes. *J. Biol. Chem. 259*, 12346–12349.
16. Miller, W. H., Daluge, S. M., Garvey, E. P., Hopkins, S., Reardon, J. E., Boyd, F. L., and Miller, R. L. (1992) Phosphorylation of Carbovir Enantiomers by Cellular Enzymes Determines the Stereoselectivity of Antiviral Activity. *J. Biol. Chem. 267*, 21220–21224.
17. Walker, J. E., Saraste, M., Runswick, M. J., and Gay, N. J. (1982) Distantly Related Sequences in the Alpha- and Beta-subunits of ATP Synthase, Myosin, Kinases and Other ATP-Requiring Enzymes and a Common Nucleotide Binding Fold. *EMBO J. 1*, 945–951.
18. Stehle, T., and Schulz, G. E. (1992) Refined Structure of the Complex between Guanylate Kinase and its Substrate GMP at 2.0 Å Resolution. *J. Mol. Biol. 224*, 1127–1141.
19. Beck, B. J., Huelsmeyer, M., Paul, S., and Downs, D. M. (2003) A Mutation in the Essential Gene gmk (Encoding Guanylate Kinase) Generates a Requirement for Adenine at Low Temperature in *Salmonella enterica*. *J. Bacteriol. 185*, 6732–6735.
20. Blaszczyk, J., Li, Y., Yan, H., and Ji, X. (2001) Crystal Structure of Unligated Guanylate Kinase from Yeast Reveals GMP-Induced Conformational Changes. *J. Mol. Biol. 307*, 242–257.
21. Zhang, Y., Li, Y., Wu, Y., and Yan, H. (1997) Structural and Functional Roles of Tyrosine 78 of Yeast Guanylate Kinase. *J. Biol. Chem. 272*, 19343–19350.
22. Pettersen, E. F., Goddard, T. D., Huang, C. C., Couch, G. S., Greenblatt, D. M., Meng, E. C., and Ferrin, T. E. (2004) UCSF Chimera - A Visualization System for Exploratory Research and Analysis. *J. Comput. Chem. 25*, 1605–1612.
23. Agarwal, K. C., Miech, R. P., and Parks, R. E.Jr. (1978) Guanylate Kinases from Human Erythrocytes, Hog Brain, and Rat Liver. *Methods Enzymol. 51*, 483–490.
24. States, D. J., Haberkorn, R. A., and Ruben, D. J. (1982) A Two-Dimensional Nuclear Overhauser Experiment with Pure Absorption Phase in Four Quadrants. *J. Magn. Reson. 48*, 286–292.
25. Macura, S., Huang, Y., Suter, D., and Ernst, R. R. (1981) Two-Dimensional chemical Exchange and Cross-Relaxation Spectroscopy of Coupled Nuclear Spins. *J. Magn. Reson. 43*, 259–281.
26. Campbell, A. P., and Sykes, B. D. (1991) Theoretical Evaluation of the Two-Dimensional Transferred Nuclear Overhauser Effect. *J. Magn. Reson. 93*, 77–92.
27. Ni, F. (1992) Complete Relaxation Matrix Analysis of Transferred Nuclear Overhauser Effects. *J. Magn. Reson. 96*, 651–656.
28. Lee, W., and Krishna, N. R. (1992) Influence of Conformational Exchange on the 2D NOESY Spectra of Biomolecules Existing in Multiple Conformations. *J. Magn. Reson. 98*, 36–48.
29. London, R. E., Perlman, M. E., and Davis, D. G. (1992) Relaxation-Matrix Analysis of the Transferred Nuclear Overhauser Effect for Finite Exchange Rates. *J. Magn. Reson. 97*, 79–98.
30. Zheng, J., and Post, C. B. (1993) Protein Indirect Relaxation Effects in Exchange-Transferred NOESY by a Rate-Matrix Analysis. *J. Magn. Reson. B 101*, 262–270.
31. Landy, S. B., and Nageswara Rao, B. D. (1989) Dynamical NOE in Multiple-Spin Systems Undergoing Chemical Exchange. *J. Magn. Reson. 81*, 371–377.
32. Abragam, A. (1961) Principles of Nuclear Magnetism , Oxford University Press, London.
33. Noggle, J. H., and Schirmer, R. E. (1971) The Nuclear Overhauser Effect , Academic Press, New York.
34. Gasteiger, J., and Marsili, M. (1980) Iterative Partial Equalization of Orbital Electronegativity—A Rapid Access To Atomic Charges. *Tetrahedron 36*, 3219–3228.
35. Marsili, M., and Gasteiger, J. (1980) Pi-Charge Distributions from Molecular Topology and Pi-Orbital Electronegativity Croat. *Chem. Acta 53*, 601–614.
36. Tian, G., Yan, H., Jiang, R.-T., Fumio, K., Nakazawa, A., and Tsai, M.-D. (1990) Mechanism of Adenylate Kinase. 6: Are the Essential Lysines Essential. *Biochemistry 29*, 4296–4304.
37. Hosur, R. V., Govil, G., and Miles, H. T. (1988) Application of 2D NMR Spectroscopy in the Determination of Solution Conformation of Nucleic Acids. *Magn. Reson. Chem. 26*, 927–944.
38. Byeon, I.-J. L., Shi, Z., and Tsai, M.-D. (1995) Mechanism of Adenylate Kinase. 18: The "Essential Lysine" Helps To Orient the Phosphates and the Active Site Residues to Proper Conformations. *Biochemistry 34*, 3172–3182.
39. Kleywegt, G. J., Henrick, K., Dodson, E. J., and van Aalten, D. M. F. (2003) Pound-Wise but Penny-Foolish: How Well Do

Micromolecules Fare in Macromolecular Refinement?. *Struct. 11*, 1051–1059.
40. Davis, A. M., Teague, S. J., and Kleywegt, G. J. (2003) Application and Limitations of X-ray Crystallographic Data in Structure-Based Ligand and Drug Design. *Angew. Chem. 42*, 2718–2736.
41. Hilber, D. W., Stolowich, N. J., Reynolds, M. A., Gerlt, J. A., Wilde, J. A., and Bolton, P. H. (1987) Site-Directed Mutants of Staphylococcal Nuclease: Detection and Localization by ^{1}H NMR Spectroscopy of Conformational Changes Accompanying Substitutions for Glutamic Acid-43. *Biochemistry 26*, 6278–6286.
42. Leipe, D. D., Koonin, E. V., and Aravind, L. (2003) Evolution and Classification of P-loop Kinases and Related Proteins. *J. Mol. Biol. 333*, 781–815.